

Deposition Mechanism of Anatase TiO₂ on Self-Assembled Monolayers from an Aqueous Solution

Y. Masuda,^{*,†} T. Sugiyama,[†] W. S. Seo,[‡] and K. Koumoto[†]

Department of Applied Chemistry, Graduate School of Engineering, Nagoya University, Nagoya 464-8603, Japan, and Korea Institute of Ceramic Engineering & Technology (KICET), Korea

Received March 5, 2003. Revised Manuscript Received April 21, 2003

The nucleation and growth process of anatase TiO₂ on several kinds of self-assembled monolayers (SAMs) in an aqueous solution has been evaluated in detail. Homogeneously nucleated TiO₂ particles and amino groups of SAM showed negative or positive ζ potential in the solution, respectively. The adhesion of TiO₂ particles to the amino group surface by attractive electrostatic interaction caused rapid growth of TiO₂ thin films in the supersaturated solution at pH 2.8. On the other hand, TiO₂ was deposited on SAMs without the adhesion of TiO₂ particles regardless of the type of SAM in the solution at pH 1.5 whose degree of supersaturation is low as a result of a high concentration of H⁺. Additionally, the orientation of films deposited on all SAMs was shown to be improved by enlarging the reaction time regardless of the kind of SAM or pH. It is conjectured that the adsorption of anions to specific crystal planes caused *c*-axis orientation of anatase TiO₂.

Introduction

Titanium dioxide (TiO₂) thin films are of interest for various applications including microelectronics,¹ optical cells,² solar energy conversion,³ highly efficient catalysts,⁴ microorganism photolysis,⁵ antifogging and self-cleaning coatings,⁶ gratings,⁷ gate oxides in MOSFETs (metal-oxide-semiconductor field effect transistor),^{8,9} etc. Accordingly, various attempts have been made to fabricate thin films and micropatterns of TiO₂ by several methods and, in particular, to synthesize materials and devices including TiO₂ thin films from an aqueous solution through an environmentally friendly synthesis process, i.e., “green chemistry”.

TiO₂ films have been prepared from aqueous solutions via various methods.^{10–19} Deki et al.^{10–13} prepared

amorphous TiO₂ thin films containing 37 vol %¹³ non-oriented anatase TiO₂ on glass substrates at 30 °C from a (NH₄)₂TiF₆ aqueous solution using liquid-phase deposition (LPD), which was first used for SiO₂.²⁰ The TiO₂ thin films were transparent because they were made of polycrystalline particles that were smaller than the wavelength of visible light. Rutile TiO₂ thin films (0.18 μ m) were also prepared on α -Al₂O₃ substrates by hydrothermal treatment of a mixed TiO₄²⁻ (0.5 M) and HNO₃ (2.0 M) solution at low temperature (100–200 °C).¹⁴ The film, consisting of short columnar grains (50 \times 20 nm²), was uniform, homogeneous, and without visible defects. TiO₂ thin films were also deposited in aqueous HCl solutions of TiCl₄ for 2 h at 80 °C on SAMs of SO₃H groups formed on glass substrates.¹⁵ TiCl₄ was hydrolyzed in an aqueous solution to produce TiO₂ particles which adhered to a substrate. The films consisted of TiO₂ crystallites around 120 nm in size.

Micropatterning of TiO₂ was attempted by a number of methods referring to these thin film fabrication processes.^{21–26} We fashioned an anatase TiO₂ thin film

* Tel: +81-52-789-3329. Fax: +81-52-789-3201. E-mail: masuda@apchem.nagoya-u.ac.jp.

[†] Nagoya University.

[‡] Korea Institute of Ceramic Engineering & Technology.

- (1) Burns, G. P. *J. Appl. Phys.* **1989**, *65*, 2095.
- (2) Yoldas, B. E.; O'Keefe, T. W. *Appl. Opt.* **1979**, *18*, 3133.
- (3) Butler, M. A.; Ginley, D. S. *J. Mater. Sci.* **1980**, *15*, 19.
- (4) Carlson, T.; Giffin, G. L. *J. Phys. Chem.* **1986**, *90*, 5896.
- (5) Matsunaga, T.; Tomoda, R.; Nakajima, T.; Komine, T. *Appl. Environ. Microbiol.* **1988**, *54*, 330.
- (6) Wang, R.; Hashimoto, K.; Fujishima, A. *Nature* **1997**, *388*, 431.
- (7) Borenstain, S. I.; Arad, U.; Lyubina, I.; Segal, A.; Warschawer, Y. *Thin Solid Films* **1999**, *75*, 2659.
- (8) Peercy, P. S. *Nature* **2000**, *406*, 1023.
- (9) Wang, D. J.; Masuda, Y.; Seo, W. S.; Koumoto, K. *Key Eng. Mater.* **2002**, *214*, 163.
- (10) Deki, S.; Aoi, Y.; Hiroi, O.; Kajinami, A. *Chem. Lett.* **1996**, *6*, 433–434.
- (11) Deki, S.; Aoi, Y.; Yanagimoto, H.; Ishii, K.; Akamatsu, K.; Mizuhata, M.; Kajinami, A. *J. Mater. Chem.* **1996**, *6*, 1879–1882.
- (12) Deki, S.; Aoi, Y.; Asaoka, Y.; Kajinami, A.; Mizuhata, M. *J. Mater. Chem.* **1997**, *7*, 733–736.
- (13) Kishimoto, H.; Takahama, K.; Hashimoto, N.; Aoi, Y.; Deki, S. *J. Mater. Chem.* **1998**, *8*, 2019–2024.
- (14) Chen, Q.; Quian, Y.; Chen, Z.; Jia, Y.; Zhou, G.; Li, X.; Zhang, Y. *Phys. Status Solidi A* **1996**, *156*, 381.

- (15) Huang, D.; Xiao, Z.-D.; Gu, J.-H.; Huang, N.-P.; Yuan, C.-W. *Thin Solid Films* **1997**, *305*, 110.
- (16) Shimizu, K.; Imai, H.; Hirashima, H.; Tsukuma, K. *Thin Solid Films* **2000**, *351*, 220.
- (17) Wang, W. P.; Yu, Y.; Hu, F. X.; Gao, L. *Thin Solid Films* **2000**, *371*, 148.
- (18) Lee, M. K.; Lei, B. H. *Jpn. J. Appl. Phys.* **2000**, *39*, 101.
- (19) Selvaraj, U.; Prasadarao, A. V.; Komarneni, S.; Roy, R. *J. Am. Ceram. Soc.* **1992**, *75* (5), 1167.
- (20) Nagayama, H.; Honda, H.; Kawahara, H. *J. Electrochem. Soc.* **1988**, *135*, 2013–2016.
- (21) Koumoto, K.; Seo, S.; Sugiyama, T.; Seo, W. S.; Dressick, W. *J. Chem. Mater.* **1999**, *11* (9), 2305.
- (22) Collins, R. J.; Shin, H.; De Guire, M. R.; Heuer, A. H.; Shukenik, C. N. *Appl. Phys. Lett.* **1996**, *69* (6), 860.
- (23) Bartz, M.; Terfort, A.; Knoll, W.; Tremel, W. *Chem. Eur. J.* **2000**, *6* (22), 4149.
- (24) Masuda, Y.; Sugiyama, T.; Lin, H.; Seo, W. S.; Koumoto, K. *Thin Solid Films* **2001**, *382*, 153.

micropattern²¹ on a patterned SAM.^{27–29} A phenyltrichlorosilane (PTCS)-SAM was irradiated by ultraviolet (UV) light through a photomask to form an OH/phenyl micropattern which was then used as a template.²¹ Anatase TiO₂ thin films were deposited on the entire area of a patterned SAM from a (NH₄)₂TiF₆ aqueous solution with the addition of H₃BO₃ at 50 °C for 6 h. Thin films on phenyl regions were then peeled off by sonication. Thin films on the OH group region showed strong adhesion to OH groups compared with those on the phenyl regions. Consequently, a micropattern of anatase TiO₂ was fabricated at low temperature. However, the lift-off process causes deterioration of the feature edge acuity of the micropattern, and a site-selective deposition process is needed to fabricate the micropattern of a TiO₂ thin film that has high feature edge acuity.

On the other hand, a micropattern of the anatase TiO₂ thin film was fabricated by the site-selective immersion³⁰ method using a SAM which has a pattern of both hydrophilic and hydrophobic surfaces. A solution containing a Ti precursor contacted the hydrophilic surface during the experiment and briefly came in contact with the hydrophobic surface. The solution on the hydrophilic surface was replaced with a fresh solution by continuous movement of bubbles. Thus, TiO₂ was deposited and a thin film was grown on the hydrophilic surface selectively. The TiO₂ thin film fabricated by the site-selective immersion method had no cracks, and the feature edge acuity of its micropattern was much higher than that of the micropattern obtained by the lift-off process.²¹

However, the feature edge acuity of the micropattern needs to be improved further in order to use anatase TiO₂ micropatterns for electronic or optical devices. Investigation of the mechanism of nucleation and growth of TiO₂ from the aqueous solution would produce valuable information for making desired thin films and micropatterns. De Guire et al.³¹ recently reported a systematic study of LPD TiO₂ film formation on silicon wafer substrates prepared by various means, assuming that homogeneously nucleated particles have a positive surface charge density at pH 2.88–3.88 in a solution containing several ions such as TiF₆²⁻ and BO₃³⁻. They showed that the growth rate and crystallinity of these films could be controlled by careful manipulation of solution parameters and the surface functionality of the substrate. Although they discussed the effects of the substrate surface functionality on TiO₂ films in detail and suggested the mechanism of the deposition process based on their experimental results, further quantitative analyses of the growth process, such as of the surface potential of SAMs and particles, deposition rate on SAMs, and time dependence of the crystal-axis

orientation of anatase TiO₂ thin films, are necessary to clarify the deposition mechanism.

In this study, we evaluated in detail the deposition process of anatase TiO₂ from an aqueous solution using a quartz crystal microbalance (QCM), an electrophoretic light-scattering spectrometer, a scanning electron microscope (SEM), and an X-ray diffractometer (XRD). We evaluated the surface ζ potential of SAMs and TiO₂ particles in a solution containing ions such as TiF₆²⁻ and BO₃³⁻. We also investigated the TiO₂ deposition rate and quantity for several kinds of SAMs and the time dependence of the crystal-axis orientation to clarify the mechanism of nucleation and growth.

Experimental Section

SAM Preparation. Octadecyltrichlorosilane (OTS-SAM) and PTCS-SAM were prepared by immersing the Si substrate (p-type Si[100]) in an anhydrous toluene solution containing 1 vol % OTS and PTCS, respectively, for 5 min under an N₂ atmosphere.^{21,24–30} (3-Aminopropyl)triethoxysilane (APTS)-SAM was prepared by immersion in an anhydrous toluene solution containing 1 vol % APTS for 1 h in air. The substrates with SAMs were baked at 120 °C for 5 min to remove residual solvent and promote chemisorption of the SAM. Octadecylmercaptan (OM)-SAM, phenylmercaptan (PM)-SAM, and 2-aminoethanethiol (AET)-SAM were prepared by immersing the Au-coated quartz crystal of a QCM (QCA917, Seiko EG&G Co., Ltd.) in a bicyclohexyl solution containing 1 vol % OM, PM, and AET, respectively, for 30 min under an N₂ atmosphere. The substrates with SAMs were then rinsed with anhydrous toluene to remove residual reagents. OM-SAM on the quartz crystal of the QCM was exposed for 2 h to UV light (184.9 nm) to assess the deposition rate of TiO₂ on OH groups.

OTS-SAM has a methyl group at the end of a long methylene chain, whereas PTCS-SAM and APTS-SAM have phenyl groups and amino groups, respectively. OM-SAM, PM-SAM, and AET-SAM have octadecyl, phenyl, and amino groups, respectively, and their functional groups are similar to those of OTS-SAM, PTCS-SAM, and APTS-SAM. They were used instead of OTS-SAM, PTCS-SAM, or APTS-SAM for QCM analysis because trichlorosilane reagents such as OTS, PTCS, and APTS cannot form SAMs on Au-coated substrates. Initially deposited OTS-SAM, PTCS-SAM, APTS-SAM, OM-SAM, PM-SAM, and AET-SAM showed water contact angles of 96°, 74°, 48°, 96°, 76°, and 53°, respectively. UV-irradiated surfaces of SAMs were, however, wetted completely (contact angle <5°). This suggests that SAMs of OTS, PTCS, APTS, OM, PM, and AET were modified to hydrophilic OH group surfaces by UV irradiation. The order of SAM hydrophobicity determined from these measurements was OTS-SAM > PTCS-SAM > APTS-SAM > OH groups on silicon. ζ potentials measured in aqueous solutions (pH 7.0) for the surface of a silicon substrate covered with OH groups, phenyl groups (PTCS), and amino groups (APTS) were measured to be -38.23, +0.63, and +22.0 mV,³² respectively. The order of ζ potentials in the aqueous solution of our experiment is presumed to be APTS-SAM > PTCS-SAM > OH-SAM (OH groups on silicon).

Deposition of TiO₂ Thin Films. Ammonium hexafluorotitanate [(NH₄)₂TiF₆] and boric acid (H₃BO₃) were separately dissolved in deionized water at 50 °C and kept for 12 h (Figure 1). An appropriate amount of HCl was added to the boric acid solution to control pH, and an ammonium hexafluorotitanate solution was added.²¹ SAMs were immersed in the solution containing 0.05 M [(NH₄)₂TiF₆] and 0.15 M H₃BO₃ at pH 1.5 or 2.8 and kept at 50 °C to deposit anatase TiO₂. Deposition of TiO₂ proceeds by the following mechanisms:^{10–13}

(25) Masuda, Y.; Seo, W. S.; Koumoto, K. *Langmuir* **2001**, *17* (16), 4876.

(26) Masuda, Y.; Jinbo, Y.; Yonezawa, T.; Koumoto, K. *Chem. Mater.* **2002**, *14* (3), 1236.

(27) Masuda, Y.; Seo, W. S.; Koumoto, K. *Thin Solid Films* **2001**, *382*, 183.

(28) Masuda, Y.; Seo, W. S.; Koumoto, K. *Jpn. J. Appl. Phys.* **2000**, *39*, 4596.

(29) Masuda, Y.; Itoh, M.; Yonezawa, T.; Koumoto, K. *Langmuir* **2002**, *18* (10), 4155–4159.

(30) Masuda, Y.; Sugiyama, T.; Koumoto, K. *J. Mater. Chem.* **2002**, *12* (9), 2643–2647.

(31) Pizem, H.; Sukenik, C. N.; Sampathkumaran, U.; McIlwain, A. K.; De Guire, M. R. *Chem. Mater.* **2002**, *14*, 2476–2485.

(32) Zhu, P. X.; Ishikawa, M.; Seo, W. S.; Koumoto, K. *J. Biomed. Mater. Res.* **2002**, *59*, 294–304.

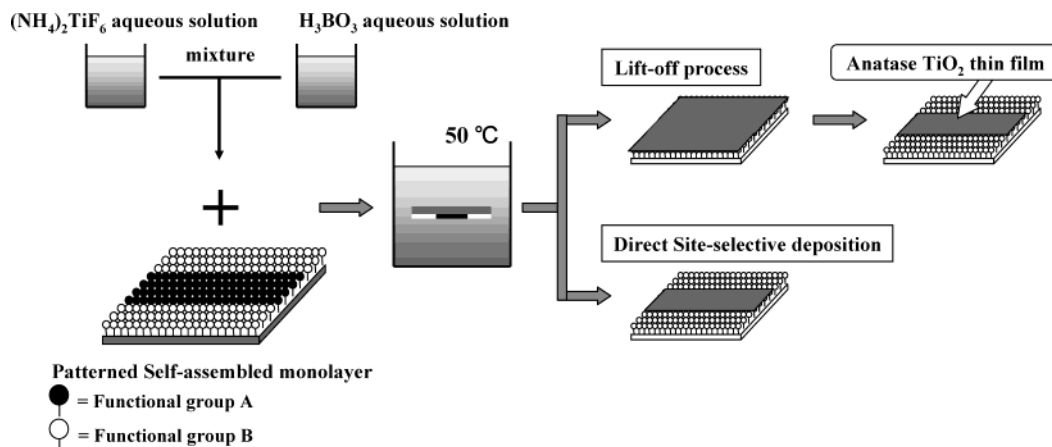
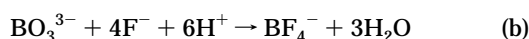
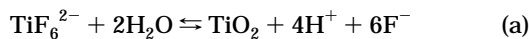


Figure 1. Conceptual process for fabricating a micropattern of anatase TiO₂ thin film from an aqueous solution.



QCM Measurement. Quartz crystals covered with SAMs were placed 5 mm below the surface of the solution. The solution was kept covered to prevent the evaporation of water, and water (50 °C) was added to compensate for any evaporated water. A frequency decrease [ΔF (Hz)] was converted into a weight increase [Δm (ng)] by the following equation:

$$\Delta m \text{ (ng)} = -1.068\Delta F \text{ (Hz)} \quad (\text{c})$$

Results and Discussion

ζ Potential of TiO₂ Particles. In the solution at pH 2.8, many homogeneously nucleated particles were deposited on the substrate and grew to form thin films because of the solution's high degree of supersaturation. It is important to understand the interactions between homogeneously nucleated particles and a substrate in order to investigate the deposition mechanism. Therefore, we evaluated the ζ potential of homogeneously nucleated TiO₂ particles in the solution.

A 0.05 M TiF₆²⁻ solution and a 0.015 M BO₃³⁻ solution were kept at 50 °C for 24 h. They were then mixed and kept at 50 °C for 30 min to grow TiO₂ particles. The surface character (ζ potential) of homogeneously nucleated anatase TiO₂ particles in the solution containing TiF₆²⁻ and BO₃³⁻ ions was examined by direct measurement of electrophoretic mobility using an electrophoretic light-scattering spectrometer (Zetasizer 3000HS, Malvern Instruments Co., Ltd.). The ζ potential of TiO₂ particles was determined to be -14 mV at pH 2.8 (Figure 2), though the isoelectric point (IEP) of TiO₂ was reported to be 2.7–6.0 (anatase),³³ 3.4–5.5 (rutile),³³ 5.6 (rutile),³⁴³⁴ 5.9 (rutile),³⁵³⁵ or 6.2 (rutile).³⁶³⁶ The ζ potential of anatase TiO₂ particles in the solution was also confirmed to be negative in these pH regions [-16.6 V at pH 3.8 (plotted in Figure 2)] with another electrophoretic light-scattering spectrophotometer (ELS-8000, Otsuka Electronics Co., Ltd.).

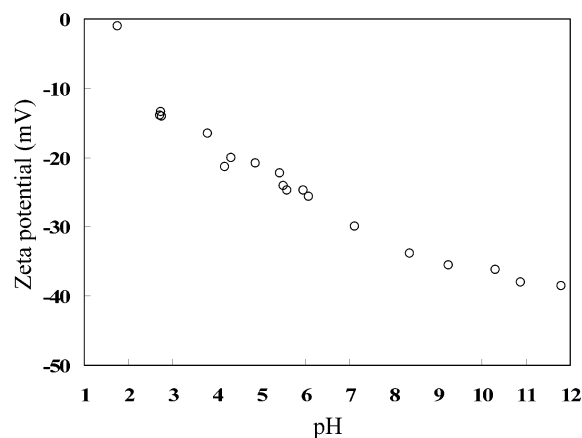


Figure 2. ζ potential of homogeneously nucleated TiO₂ particles in the solution containing TiF₆²⁻ and BO₃³⁻ ions.

The ζ potential is very sensitive to the surface conditions of particles, ions adsorbed on the particle surfaces, and the kinds and concentrations of ions in the solution. The variations in the ζ potential were likely caused by the difference in the surface conditions of TiO₂ particles affected by the interactions between particles and ions in the solution.

The adsorption of ions which affect the ζ potential was observed in HCl,³⁷ KCl,³⁷ BaCl₂,³⁷ KOH,³⁷ dodecyltrimethylammonium bromide,³⁸ and sodium dodecyl sulfate (SDS)³⁸ aqueous solutions. The ζ potential of rutile in pure water was -17 mV (IEP pH 4.5) and decreased with the addition of SDS to -43 mV (SDS: 1 mM).³⁸ It is concluded that DS⁻ ions (C₁₂H₂₅OSO₃⁻) replaced hydroxyl ions (HO⁻) on the surface of rutile to decrease the ζ potential. The effect of anions should be more pronounced than that of cations under the conditions in our study.

Additionally, the ζ potential of rutile treated at 1000 °C was -18 mV in pure water and decreased with the addition of sodium triphosphate to -53 mV (4 × 10⁴ equiv/L).³⁷ The positively charged surfaces in water were all inverted by the addition of triphosphate, and the negatively charged rutile surface became more negative, even at an extremely low concentration of

(33) Furlong, D. N.; Parfitt, G. D. *J. Colloid Interface Sci.* **1978**, *65*, 548–554.

(34) Larson, I.; Drummond, C. J.; Chan, D. Y. C.; Grieser, F. J. *Am. Chem. Soc.* **1993**, *115*, 11885.

(35) Wiese, G. R.; Healy, T. W. *J. Colloid Interface Sci.* **1975**, *51*, 427–433.

(36) Yotsumoto, H.; Yoon, R. H. *J. Colloid Interface Sci.* **1993**, *157*, 426.

(37) Morimoto, T.; Sakamoto, M. *Bull. Chem. Soc. Jpn.* **1964**, *37* (5), 719–723.

(38) Parfitt, G. D.; Wharton, D. G. *J. Colloid Interface Sci.* **1972**, *38* (2), 431–439.

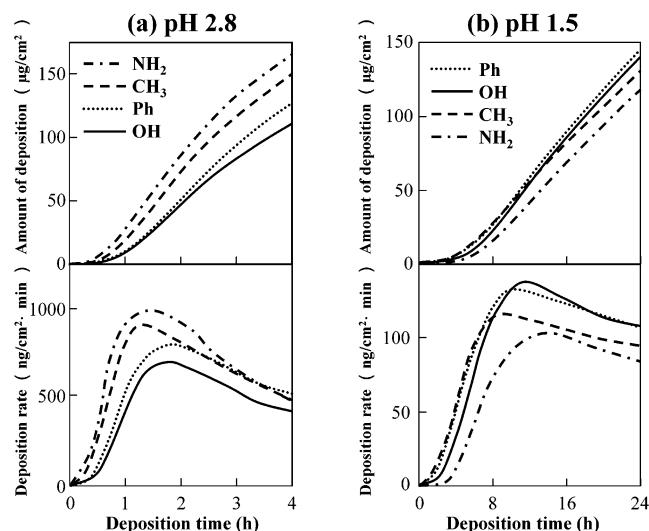


Figure 3. Deposition rate and deposition quantity of TiO₂ in the solution at (a) pH 2.8 or (b) pH 1.5 as a function of the deposition time.

triphosphate. This was obviously caused by the strong adsorption of triphosphate, suggesting the formation of a complex compound on the surface of TiO₂.³⁷ These findings reported in the literature strongly support our conjecture that anions must have adsorbed to the surfaces of TiO₂ particles, giving rise to highly negative ζ potential because many kinds of anions, such as F⁻, BO₃³⁻, BF₄⁻, and TiF₆²⁻, were contained in our solution with a concentration of more than 2×10^{-2} M.³⁶

We have reported that negatively charged microparticles of hydroxyapatite were drawn to attach to a positive silicon surface covered by amino groups owing to an attractive electrostatic force, whereas no particles were observed on a negatively charged silicon surface covered by OH groups.³² We therefore evaluated the deposition rates for several kinds of SAMs at pH 2.8.

Nucleation and Crystal Growth of TiO₂ on SAMs. SAMs of OM-SAM, PM-SAM, AET-SAM, and UV-irradiated OM-SAM (OH-SAM) were immersed in the solution containing 0.05 M TiF₆²⁻ and 0.015 M BO₃³⁻ at pH 1.5 (Figure 3a) and pH 2.8 (Figure 3b) to evaluate the reaction rate on SAMs in the solution. The degree of supersaturation is high at pH 2.8 because a low H⁺ concentration promotes TiO₂ generation as indicated by eq a. Thus, many homogeneously nucleated TiO₂ particles were observed in the solution. Although no significant variation in the induction time was observed among these SAMs, the deposition rate on AET(NH₂)-SAM was much higher than that on OH-SAM (OH groups) and showed the following order: APTS (AET)-SAM > OTS (OM)-SAM > PTCS (PM)-SAM > OH-SAM (Figure 3a). This order of the deposition rate is similar to that of the ζ potential of SAMs, indicating that negatively charged TiO₂ particles are definitely attracted to positively charged SAMs by the attractive electrostatic interaction and form a TiO₂ film. Accordingly, the amount of TiO₂ deposited on OH-SAM was less than that on APTS (AET)-SAM.

On the other hand, no significant variation in the amount of deposition and deposition rates was observed among the four SAMs at pH 1.5 (Figure 3b). The solution was transparent during the whole experiment. The supersaturation degree of the solution at pH 1.5

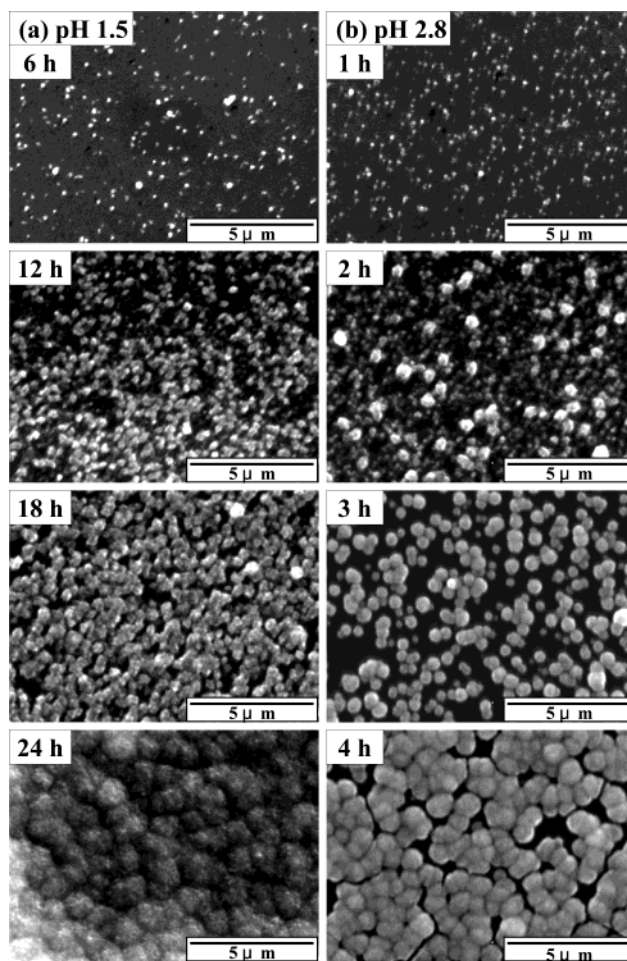


Figure 4. SEM micrographs of (a) TiO₂ on OH groups deposited for 6, 12, 18, or 24 h in the solution at pH 1.5 and (b) TiO₂ on OH groups deposited for 1, 2, 3, or 4 h in the solution at pH 2.8.

was low as a result of the high concentration of H⁺ which suppressed the deposition of TiO₂. TiO₂ is probably deposited mainly by heterogeneous nucleation in this solution, and nucleation and growth events are scarcely affected by surface functional groups of SAMs. This suggests that the critical free energies for heterogeneous nucleation of anatase TiO₂ may be similar for the SAMs employed here. Additionally, TiO₂ probably grew on pinholes and other defects in SAMs as reported^{39–44} because they can act as nucleation sites for TiO₂ growth. As the deposition was carried out at elevated temperature (50 °C), it is likely that pinholes and defects continuously opened and closed on SAM surfaces because of the thermal motions of organic groups in these films.

Moreover, the numerical density of particles and the particle size were measured directly from SEM micrographs (S-3000N, Hitachi, Ltd.; Figure 4). The particle

(39) Gun, J.; Sagiv, J. *J. Colloid Interface Sci.* **1986**, *112*, 457–472.
(40) McGovern, M. E.; Kallury, K. M. R.; Thompson, M. *Langmuir* **1994**, *10*, 3607–3614.

(41) Duchet, J.; Chabert, B.; Chapel, J. P.; Gerard, J. F.; Chevillon, J. M.; Jaffrezic-Renault, N. *Langmuir* **1997**, *13*, 2271–2278.

(42) Dressick, W. J.; Chen, M.-S.; Brandow, S. L. *J. Am. Chem. Soc.* **2000**, *122*, 982–983.

(43) Dressick, W. J.; Chen, M.-S.; Brandow, S. L.; Rhee, K. W.; Shirey, L. M.; Perkins, F. K. *Appl. Phys. Lett.* **2001**, *78*, 676–678.

(44) Dressick, W. J.; Nealey, P. F.; Brandow, S. L. *Proc. SPIE* **2001**, *4343*, 294–305.

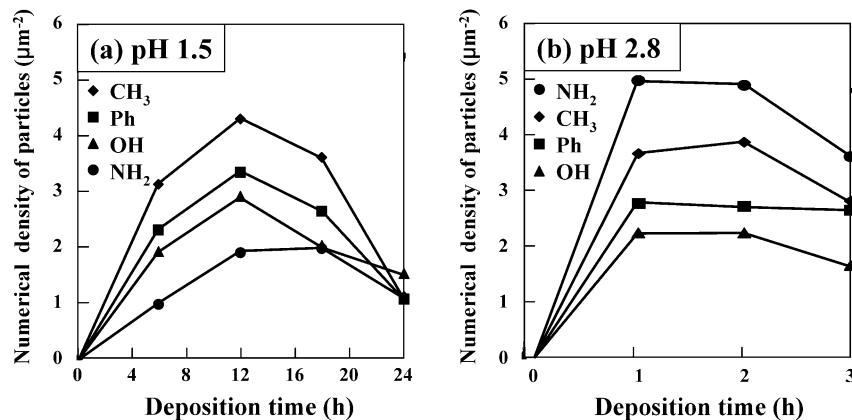


Figure 5. Numerical density of TiO₂ particles on SAMs which have phenyl, methyl, OH, or amino groups in the solution at (a) pH 1.5 or (b) pH 2.8 as a function of the deposition time.

size on the OH-group surface nearly equaled that on other SAMs, although the particle size on OTS-SAM was slightly smaller than that on the OH-group surface at pH 1.5. Whereas the particle size on each SAM increased with the reaction time [240 nm (6 h), 380 nm (12 h), 530 nm (18 h), and 1100 nm (24 h) at pH 1.5 and 400 nm (1 h), 480 nm (2 h), 770 nm (3 h), and 960 nm (4 h) at pH 2.8], the numerical density of particles reached a maximum after 10–16 h of reaction at pH 1.5 or after 1–2 h of reaction at pH 2.8 (Figure 5). This shows that small particles were incorporated into large particles because they began to contact each other after these periods. The difference in the amount of deposition determined from QCM measurements did not stem from particle size variations but from particle density. The order of the particle numerical density at pH 2.8 (NH₂ > CH₃ > Ph > OH) (Figure 5b) agrees with the order of the amount of deposition at pH 2.8 measured by QCM (Figure 3b).

Deposition processes in solutions at pH 1.26, 1.72, 2.22, and 3.75 were further studied, but no marked difference in the deposition behavior was observed. The dissimilarity in either the ζ potential or hydrophobicity of SAMs showed no salient difference in the deposition behavior in our solution.

Crystal-Axis Orientation of the TiO₂ Thin Film.

The growth process of TiO₂ thin films and the crystal-axis orientation changes were investigated using an XRD (RAD-C, Rigaku) with Cu K α radiation (40 kV and 30 mA) and a Ni filter plus a graphite monochromator. Deposited films on all SAMs showed XRD patterns of anatase TiO₂ after 24 h at pH 1.5 or after 4 h at pH 2.8. XRD patterns showed the same tendency regardless of the type of SAM, and the intensities of (004) and (105) peaks on all SAMs increased with the deposition time faster than they did for other peaks (Figure 6). The degree of crystal-axis orientation (f) was evaluated using the Lotgering method⁴⁵ taking into account the following diffraction peaks: (101) = 25.3°, (004) = 37.8°, (200) = 48.0°, (105) = 53.9°, (204) = 62.7°, (116) = 68.8°, (215) = 75.0° (Figure 7).

$$f = \frac{P - P_0}{1 - P_0} \quad (d)$$

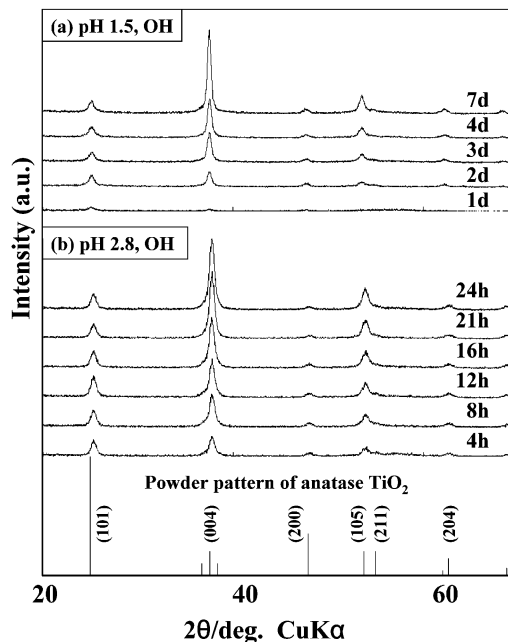


Figure 6. XRD patterns of anatase TiO₂ deposited onto OH groups in the solution at pH 2.8 as a function of the deposition time. A randomly oriented powder pattern for anatase (JCPDS card no. 21-1272) is shown for comparison.

$$P = \frac{\sum I(00l)}{\sum I(hkl)} \quad (e)$$

where P is calculated for the oriented sample and P_0 is P for the nonoriented sample (JCPDS card).

The c -axis (00 l) orientation of the film was enhanced by increasing the reaction time for all kinds of SAMs and pH (Figure 7a,b). This result suggests that the orientation of the film is determined not at the initial nucleation or deposition stage but at the film growth stage. The intensity of the (004) peak quickly increased but that of (105) increased only gradually with reaction time, and the intensities of the (101) and (200) peaks decreased after reaching their maxima regardless of the type of SAM or pH condition (Figure 7c).

Furthermore, the orientation of thin film deposited at pH 2.8 for 4 h was evaluated by a field emission SEM (FE-SEM; JSM-6700F, point-to-point resolution 1 nm,

(45) Lotgering, F. K. *J. Inorg. Nucl. Chem.* **1959**, *9*, 113–123.

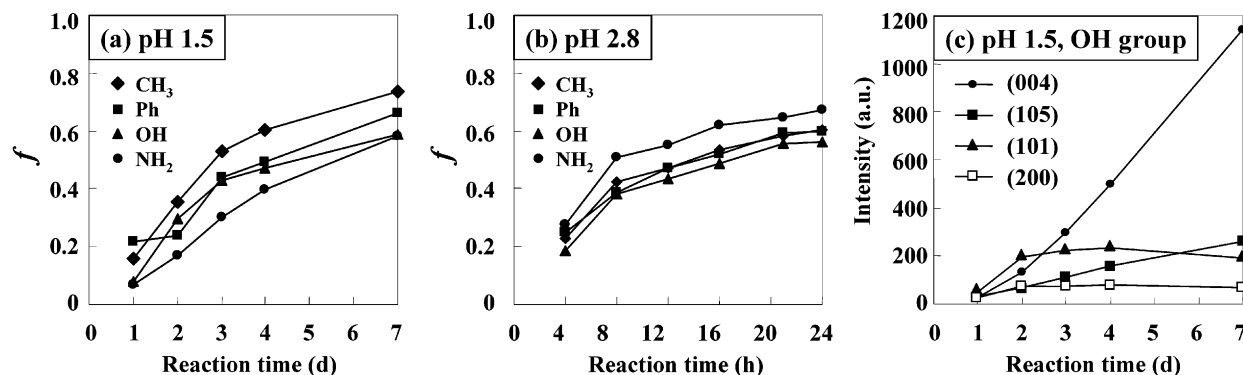


Figure 7. f (the degree of crystal-axis orientation) of anatase TiO_2 thin films deposited from the solution at (a) pH 1.5 or (b) pH 2.8 and (c) intensities of peaks as a function of the reaction time (at pH 1.5 on OH groups).

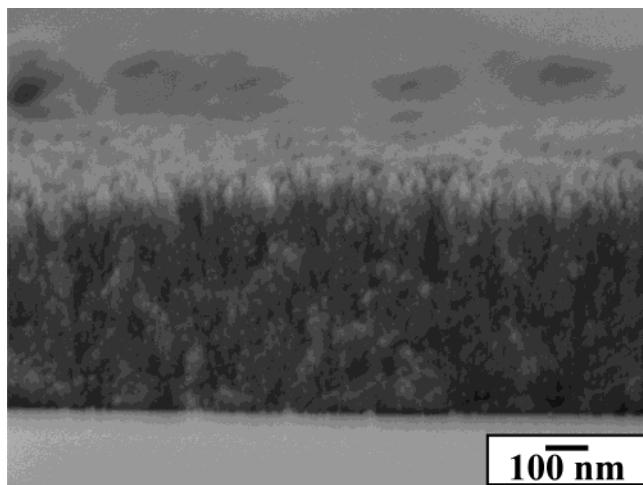


Figure 8. FE-SEM micrograph for a cross-sectional profile of the TiO_2 thin film deposited at pH 2.8.

JEOL Co., Ltd.) and a transmission electron microscope (TEM; JEM4010, 400 kV, point-to-point resolution 0.15 nm, JEOL Co., Ltd.). The cross-sectional profile of TiO_2 thin films showed columnar morphology (Figure 8). However, the columns were not clearly identified compared with the needlelike morphology of TiO_2 thin films reported recently.^{46,47} This columnar morphology is consistent with the XRD measurement which showed weak c -axis orientation (Figure 6; pH 2.8, 4 h). Figure 9 shows a TEM micrograph and electron diffraction pattern for the cross-sectional profile of a TiO_2 thin film. Many small crystals of anatase TiO_2 were observed throughout the thin film. The electron diffraction pattern also showed a weak orientation of anatase TiO_2 crystals.

These observations firmly indicate that TiO_2 particles whose c axes were perpendicular to the substrate surface may have grown faster than other crystals. Hence, the diffraction intensities of crystal planes almost perpendicular to the c axis such as (004) and (105) increased with the deposition time (Figure 7). These particles then consumed other particles whose c axis was far from perpendicular to the substrate, thus lowering the diffraction intensities of crystal planes such as (101) and (200).

This phenomenon is plausible if the (00 l) surface of an anatase crystal possesses the lowest energy compared to other crystallographic surfaces. However, the (002) surface has a high Gibbs free energy, and the (110) plane has the lowest Gibbs free energy.⁴⁸ In general, the crystal plane with the lowest Gibbs free energy will grow preferentially; that is, the preferred orientation is the one having the lowest surface free energy. Hence, the preferred orientation should be (110) in the condition without any influence on crystal orientation in which atomic diffusion is more significant, and the preferred orientation is affected more by thermodynamic factors. From these facts, the crystal growth of TiO_2 is considered to be controlled by some other factors.

De Guire et al.³¹ suggested that the selective adsorption of ions occurs on specific surfaces of anatase crystals. Oriented films do not always need oriented nucleation. The film can have an oriented fiber structure if crystals grow anisotropically. Preferential adsorption of ionic or polymeric species from the solution onto certain crystallographic faces induces anisotropic growth. The elongated growth tendency of the crystals shown in Figure 8 indicates that such growth anisotropy exists in our films. Additionally, the growth and crystallinity of anatase were discussed based on a systematic study of LPD TiO_2 films.³¹ Growth via attachment of particles is usually associated with high growth rate but also high roughness and reduced crystallographic orientation. However, De Guire et al. concluded that our method^{21,30} provides anatase TiO_2 thin films with a high growth rate, high crystallinity, and the smoothest surfaces in their comparative experiments.³¹

The adsorption of anions to anatase surfaces and its influence on the preferred orientation were discussed by Yamabi and Imai.^{46,47} The anatase TiO_2 films deposited from a TiOSO_4 solution containing urea and from a TiF_4 solution were composed of fine needles perpendicular to the substrate. The selective adsorption of coexisting species, such as SO_4^{2-} and F^- , on specific surfaces parallel to the c axis inhibits the crystal growth perpendicular to the c axis. In contrast, a randomly oriented uniform film consisting of fine spherical crys-

(48) Leng, Y. X.; Huang, N.; Yang, P.; Chen, J. Y.; Sun, H.; Wang, J.; Wan, G. J.; Tian, X. B.; Fu, R. K. Y.; Wang, L. P.; Chu, P. K. *Sci. Coating Technol.* **2002**, *156*, 295–300.

(49) Wyckoff, R. W. G. *Crystal Structures*, 2nd ed.; Interscience: New York, 1963; Vol. 1.

(50) Wells, A. F. *Structural Inorganic Chemistry*, 5th ed.; University Press: Oxford, 1975.

(46) Yamabi, S.; Imai, H. *Chem. Mater.* **2002**, *14*, 609–614.

(47) Shimizu, K.; Imai, H.; Hirashima, H.; Tsukuma, K. *Thin Solid Films* **1999**, *351*, 220–224.

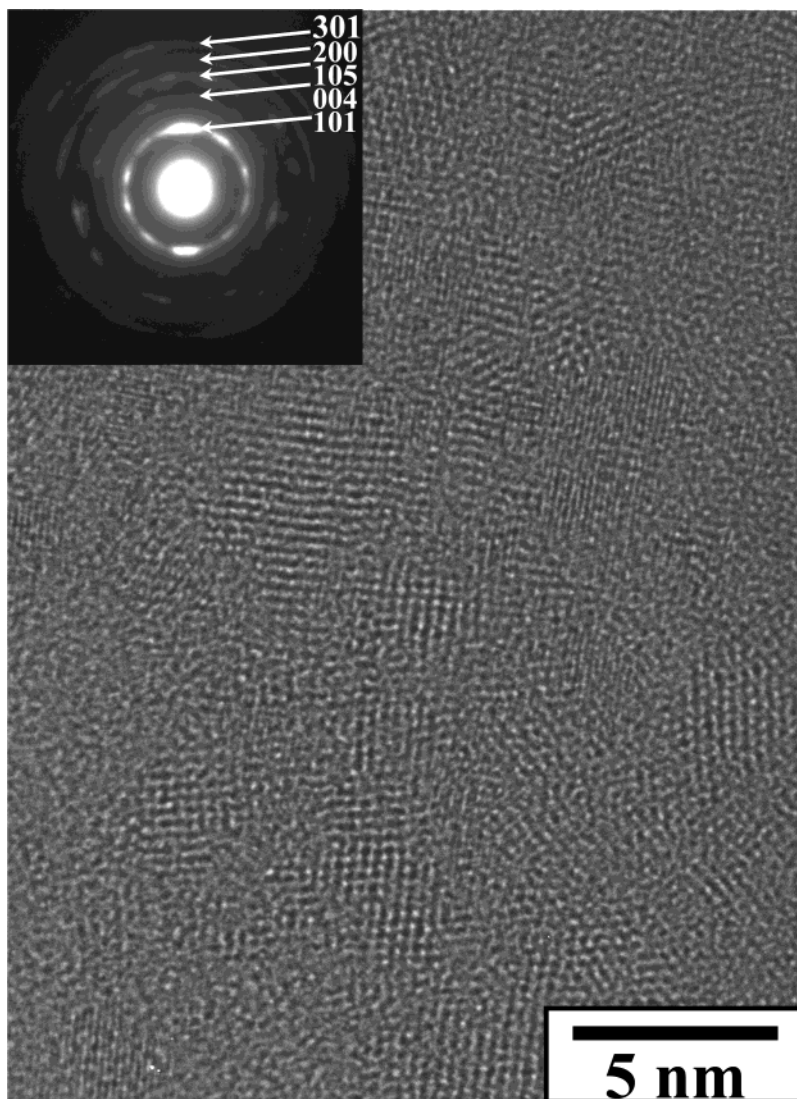


Figure 9. TEM micrograph and electron diffraction pattern for a cross-sectional profile of the TiO₂ thin film deposited at pH 2.8.

tallites with diameters of 10–20 nm was deposited from the TiOSO₄ solution without urea.⁴⁶ A high reaction rate compared with a TiOSO₄ solution containing urea⁴⁶ or a TiF₄ solution⁴⁷ induces the random orientation of spherical particles.

Likewise, many kinds of anions, such as F⁻, BO₃³⁻, BF₄⁻, and TiF₆²⁻, were included in our solution, and these would adsorb to the surfaces parallel to the *c* axis, inhibiting the growth in the direction perpendicular to the *c* axis. The anatase crystals probably grow in the *c*-axis direction. The initial nuclei which have *c* axes parallel to the substrate cannot grow fast because of the presence of neighboring particles, but in contrast the particles which have *c* axes perpendicular to the substrate can grow fast in the direction perpendicular to the substrate. Particles probably grow in the direction perpendicular to the substrate and give rise to columnar morphology, as shown in Figure 8a, which would have caused the high degree of the (00*l*) plane perpendicular to the substrate.

Conclusions

The nucleation and growth process of anatase TiO₂ on several kinds of SAMs in an aqueous solution has

been evaluated in detail. Homogeneously nucleated TiO₂ particles and amino groups of SAM showed negative or positive ζ potential in the solution, respectively. The adhesion of TiO₂ particles to the amino group surface by attractive electrostatic interaction would cause rapid growth of TiO₂ thin films in the supersaturated solution at pH 2.8. On the other hand, TiO₂ was deposited on SAMs without the adhesion of TiO₂ particles regardless of the type of SAM in the solution at pH 1.5 whose supersaturation degree was low as a result of the high concentration of H⁺. Furthermore, the crystal-axis orientation of films deposited on substrates was shown to be improved by changing the reaction time. TiO₂ crystals whose *c* axes were perpendicular to the substrate surface may have grown faster than other crystals possibly because of the selective adsorption of the coexisting species, such as F⁻, BO₃³⁻, BF₄⁻, or TiF₆²⁻, on specific surfaces parallel to the *c* axis. The growth via attachment of particles is usually associated with high growth rate but also high roughness and reduced crystallographic orientation. However, our method avoided this compromise, yielding a high growth rate as well as partial crystallographic orientation and smooth surfaces.

Acknowledgment. This work was partly supported by Grants-in-Aid for Scientific Research (Grant-in-Aid for Young Scientists No. 14703025, Exploratory Research No. 14655239) from the Ministry of Education,

Culture, Sports, Science and Technology granted to Y. Masuda.

CM030255M